Received: 8 September 2018 | Revised: 1 March 2019 | Accepted: 13 March 2019

DOI: 10.1002/elsc.201800149

Engineering in Life Sciences

RESEARCH ARTICLE

A novel LED-based 2D-fluorescence spectroscopy system for in-line monitoring of Chinese hamster ovary cell cultivations – Part I

Alexander Graf[1,2] | Jens Claßen[3] | Dörte Solle[3] | Bernd Hitzmann[4] | Karsten Rebner[2] | Marek Hoehse[1]

[1]R&D Spectroscopy & Chemometrics, Sartorius Stedim Biotech GmbH, Göttingen, Germany

[2]Process Analysis and Technology (PA&T), Faculty Applied Chemistry, Reutlingen University, Reutlingen, Germany

[3]Institute of Technical Chemistry, Gottfried Wilhelm Leibnitz University of Hanover, Hanover, Germany

[4]Process Analytics and Cereal Science, Institute of Food Science and Biotechnology, University Hohenheim, Stuttgart, Germany

Correspondence
Alexander Graf, R&D Spectroscopy & Chemometrics, Sartorius Stedim Biotech GmbH, August-Spindler-Str. 11, 37079 Göttingen, Germany.
Email: Alexander.Graf@sartorius.com

A new two-dimensional fluorescence sensor system was developed for in-line monitoring of mammalian cell cultures. Fluorescence spectroscopy allows for the detection and quantification of naturally occurring intra- and extracellular fluorophores in the cell broth. The fluorescence signals correlate to the cells' current redox state and other relevant process parameters. Cell culture pretests with twelve different excitation wavelengths showed that only three wavelengths account for a vast majority of spectral variation. Accordingly, the newly developed device utilizes three high-power LEDs as excitation sources in combination with a back-thinned CCD-spectrometer for fluorescence detection. This setup was first tested in a lab design of experiments study with process relevant fluorophores proving its suitability for cell culture monitoring with LOD in the μg/L range. The sensor was then integrated into a CHO-K1 cell culture process. The acquired fluorescence spectra of several batches were evaluated using multivariate methods. The resulting batch evolution models were challenged in deviating and "golden batch" validation runs. These first tests showed that the new sensor can trace the cells' metabolic state in a fast and reliable manner. Cellular distress is quickly detected as a deviation from the "golden batch".

KEYWORDS

2D-fluorescence spectroscopy, CHO cell cultivation, in-line bioprocess monitoring, metabolism monitoring, MVDA, PAT

1 | INTRODUCTION

For a complete implementation of quality by design (QbD) to a biopharmaceutical production process, Process Analytical Technologies (PAT) play a crucial role. As only continuous surveillance of the Design Space ensures constant product quality, in-line and non-invasive techniques are of particular interest. Here, spectroscopic methods have proven to be of great value, i.e., Raman-, Infrared- and Fluorescence-Spectroscopy [1,2].

Fluorescence spectroscopy is well established in analytical applications, and for more than thirty years, it has been investigated for its bioprocess monitoring capabilities [3,4]. The main advantage of this sensing type is that only the newly generated photons are measured and therefore do not compete against a background signal. This effect results in exceptional sensitivity with very low detection limits as well as a wide dynamic range. Moreover, fluorescence spectroscopy has fast response times and the capability of remote sensing [5]. Therefore, this method is perfectly suited for

Abbreviations: 2DF, two-dimensional fluorescence; CHO, Chinese Hamster Ovary; DoE, Design of Experiments; OPLS, orthogonal projections to latent structures; PAT, process analytical technology; PCA, principal component analysis; QbD, quality by design.

TABLE 1 Approximated excitation and emission peak wavelengths of natural fluorophores found in bioprocesses [14–18]

Classification	Fluorophore	Exc. Wl.	Emm. Wl.
Amino Acids	Trp	280, 290	350
	Tyr	275/280	300, 330–350
	Phe	260	280
Co-Enzymes	FAD, Flavines	450	515, 535
	NADH	290, 350	440, 460
Vitamins	Pyridoxin	332, 340	390, 400
	Vitamin A	325	510
	Riboflavin	370, 440	520, 530

in-line PAT applications. Several intrinsic fluorophores can be found in the bioprocess broth (Table 1. These are part of the cells' metabolism and protein production. Therefore they correlate with the cells' redox state and other critical process parameters. One early discovery of biomonitoring studies showed a direct correlation between culture fluorescence and its biomass [4]. Since then this spectroscopy type has also been used for prediction of other parameters like protein yield, glucose and amino acid concentration [3].

In most previous publications, the BioView® sensor (Delta Light & Optics, Denmark) was used. This device yields 2D-fluorescence maps in a fast and continuous matter directly in the bioreactor and is therefore suited for process monitoring. On the downside, the system uses filters for excitation and emission wavelength selection, which limits its sensitivity and dynamic range [6–8]. Moreover, due to the wear of moving parts and filter aging the operating life of the device is reduced. The numerous excitation wavelengths make the BioView® well suited for various applications. In bioprocess application, this results in the majority of the recorded data being redundant or without any information. Last, the BioView® sensor has been discontinued by the manufacturer.

For these reasons a new 2D fluorescence system has been developed that aims at in-line monitoring of mammalian cell cultures. Here, a different approach with specific LEDs for excitation and a back-thinned CCD spectrometer in combination with a newly designed probe were chosen. This setup has the advantage of simultaneous measurement of all emission-wavelengths with improved sensitivity and dynamic range. This study aimed to evaluate the new sensor's capabilities and to show its suitability for the in-line monitoring of mammalian cell cultures.

2 | MATERIALS AND METHODS

2.1 | New LED-based 2DF sensor

The new 2DF device consists of two parts: the sensor itself and a specially designed probe (Figure 1). The sensor-part can

PRACTICAL APPLICATION

The use of spectroscopic sensors for bioprocess monitoring is a powerful tool within the process analytical technology (PAT) initiative of the Food and Drug Administration. In-Line measurements are particularly important during cost-intensive manufacturing of biopharmaceuticals in order to facilitate early process fault detection, real-time product release and minimize the risk of contamination. As shown in this research article, the newly developed LED-based 2D-fluorescence spectrometer is a highly sensitive PAT tool for monitoring mammalian cell culture processes. The system enables a deep insight into the bioreactor and provides information about the cell concentration, cell viability, cell metabolism and cellular respiration within the cultivation. In summary, this research article demonstrates the great potential of the new device for bioprocess monitoring and for implementation of the PAT concept.

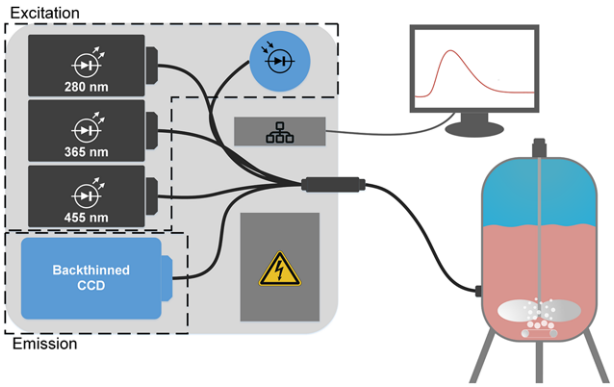

FIGURE 1 New fluorescence device set-up scheme

be further divided into two sub-sections: an excitation and a detection side. The excitation part consists of three high power LEDs (Omicron-Laserage Laserprodukte GmbH, Germany) with peak wavelengths at 280 nm, 365 nm, and 455 nm respectively and full widths at half maximum (FWHM) between 10 and 16 nm. Each LED is individually controlled, and sequential excitation makes a multiplexer redundant. From each LED a bundle of optical fibers connects to the probe head. At the same time, one fiber from each LED is connected to a photodiode for light output feedback control. For the same reason, the LEDs are initially only run at about 50% of their maximum power to have a suitable margin to counteract aging effects and ensure cross-batch comparability of the measurements.

The detection part of the system consists of a back-thinned CCD-spectrometer (Tidas OEM 800, J&M Analytik AG, Germany). This sensor obtains high sensitivity spectra over

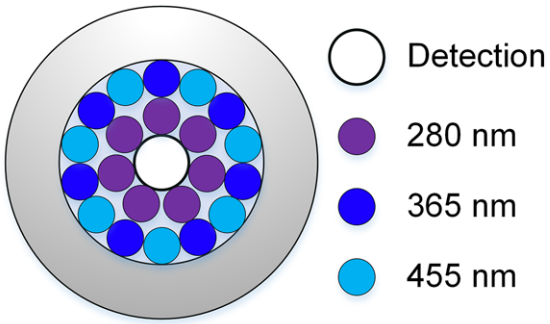

FIGURE 2 Fiber arrangement in newly designed probe

the whole UV/VIS-range (190-980 nm) with a spectral resolution < 4 nm. The whole system is controlled via the TIDASDAQ software (J&M Analytik AG, Germany) which also supports custom scripting of individual measurement protocols.

The probe head (art photonics GmbH, Germany) is inserted into the bioreactor via Ingold® port and sterilized in situ. The larger detection-fiber, which is connected to the CCD-spectrometer, is located in the probe's center. The detection fiber is first circled by the 280 nm excitation fibers. Around this inner ring, the fibers from the other two LEDs are circularly arranged in alternating order (Figure 2. This particular fiber arrangement ensures homogenous sample illumination independent of circular orientation and as mentioned before, makes the use of a multiplexer obsolete.

2.2 | BioView® sensor

The BioView® sensor consists of a classical photometric design with a Xe-lamp for excitation and a photomultiplier for emission light measurements. Emission/excitation wavelength combinations are created by two filter wheels for each the excitation and emission wavelengths respectively. Each filter wheel can hold up to sixteen filters and were set up with filters from 270–550 nm for excitation and 310–590 nm for emission selection, each with 20 nm steps in between filters. The sensor is connected via optical fibers to a probe that is inserted directly into the bioreactor [9].

2.3 | Data acquisition

During a measurement cycle, first, a dark spectrum is collected. Afterward, the first LED is turned on. The collection of the fluorescence spectrum is initiated once the controlled LED intensity reaches stability. After collection of the fluorescence spectrum, the dark spectrum is automatically redacted from it, and the LED is turned off again. The cycle is then repeated for the second and third excitation wavelength, respectively. This consecutive loop is reiterated periodically at a user-defined interval.

TABLE 2 Analytes and their concentration ranges used for DoE study

Analyte	Min. Conc.	Max. Conc	Unit	Reference
BSA	0.05	1	g/L	–
FAD	0.0025	0.05	mg/L	[19,20]
NADH	0.0325	0.65	mg/L	[19,21]
NAD	1	20	mg/L	[21]
Pyridoxine	0.0075	0.15	mg/L	–
Riboflavin	0.0075	0.15	mg/L	[20]

2.4 | Data evaluation

DoE and cultivation data were treated similarly: The already dark-corrected spectra from each excitation-wavelength were first horizontally fused with the help of Easy Analytics 1.1 (Sartorius Stedim Data Analytics AB, Sweden). Afterward, the merged data were directly imported into Simca 15 (Sartorius Stedim Data Analytics AB, Sweden). Besides mean centering, no further corrections or filtering was applied. Saturated wavelengths caused by Rayleigh scattering were excluded from the data set. The unsaturated flanks of the Rayleigh back-scattering were not excluded as they add information on cell parameters. Qualitative and quantitative models were generated using Principal Component Analysis (PCA)- and orthogonal projections to latent structures (OPLS)®-algorithms. In the case of OPLS, analyte concentrations or batch age as y-variables, respectively. The number of components was kept to a minimum to avoid overfitting while aiming for high Q^2 and low, but similar RMSEE and RMESCv.

2.5 | DoE

For a first evaluation of the sensor's capabilities, limit of detection and accuracy were determined in a design of experiment study on essential fluorophores typical for mammalian cell cultures. BSA as a target-protein replacement, FAD, NAD and NADH as co-enzymes plus pyridoxine and riboflavin of the vitamin-group were included. Concentration ranges were chosen according to concentrations in mammalian cultivations (Table 2). A benchmark test was performed by measuring the same DoE with a state of the art 2D fluorescence process instrument, the BioView® sensor.

A minimum of 5 concentrations levels has to be considered to build reliable quantitative PLS models. For three variables there are 3^5 combinations of concentrations possible. Out of these 243 combinations, five combinations are taken randomly where each variable was represented in five different concentration levels. The explained variance of the third principal component of a PCA of that five by three matrix has to be as high as possible for linear independent concentration combinations.

A brute force algorithm was used to build up three blocks of such linear independent concentration levels. By this, each variable was set at each concentration level three-fold with different concentrations of the secondary components. These 15 combinations were completed by four central experiments with an equal concentration distribution on a mean level for each variable. To determine the overall measurement error these central experiments are distributed over the whole experimental plan separating the linear independent blocks.

All solutions were prepared independently and measured under equal experimental conditions. If reliable PLS models can be built on these spectral data, the evaluated parameters are directly detected with negligible cross sensitivity.

2.6 | Cultivations

CHO cultivations were performed at TCI Hanover. A 10L BIOSTAT® Cplus bioreactor (Sartorius Stedim Biotech GmbH, Germany; T = 37°C, pH = 7.1, dO_2 = 40%, stirrer = 100 – 200 rpm) with a working volume of 7.5 L was used. CHO-K1 cells (University of Bielefeld, Germany) were grown in CHOMACS CD, chemically defined, serum-free medium (Milteny Biotec, Germany). The medium was supplemented with glutamine (8 mM end concentration). Seed-cultures were each grown in three steps in standard shake flasks inside an incubator (T = 37°C, CO_2 = 5%, rotation = 150 rpm). Inoculation was performed when cells reached a viable cell density of 6 - 10 × 10^6 cells/mL. This resulted in a starting concentration of approximately 0.4 × 10^6 viable cells/mL. For feeding, two different strategies were used. During the first three fed-batch cultivations (K1-K3), 150 mL CHOMACS feed medium (Miltenyi Biotec GmbH, Germany) that was supplemented to a final concentration of 20 g/L glucose and 37 mM glutamine, was fed every 24h, beginning 48h after inoculation. During the remaining cultures (K4 + K5), an additional automated feed was implemented. Here, whenever an at-line BioPAT® Trace analyzer (Sartorius Stedim Biotech GmbH, Germany) recognized that the glucose level dropped below 1 g/L feed medium was added. Oxygen was supplied via ring sparger with an air-oxygen mixture, in combination with a Rushton turbine for agitation. The pH-level was kept at the set point through automated addition of either 1 M sodium carbonate or by aeration with CO_2. Offline-samples were taken manually once a day and additionally every four hours with an auto-sampler (TCI Hanover, Germany). Concentrations of glucose, glutamine, glutamate, and lactate were measured once a day with a YSI 2950 biochemistry analyzer (YSI Inc., USA). Total and viable cell concentration, along with viability was quantified with a CedexHiRes (Roche AG, Germany). The cultivations were terminated whenever the cell viability dropped below 60% to investigate the effect of dying cells on the fluorescence signal.

3 | RESULTS AND DISCUSSION

3.1 | DoE

First, a DoE study was carried out with both the newly developed and a BioView® sensor to evaluate the new device's ability for process monitoring and to have a direct comparison to a state of the art instrument. Typical fluorophores of cell culture processes served as test substances.

Multivariate Analysis showed excellent prediction capabilities for BSA and Riboflavin. The accuracy was slightly lower for NADH. Pyridoxine was still well predictable when limiting the number of LVs to a reasonable number. NAD and FAD were not predictable (Figure 3).

The poor results for NAD and FAD can easily be explained. As NAD does not absorb light at 365 nm and only very little at 280 nm, its fluorescence emission is correspondingly low [10]. Since its emission signal is the same as NADH's, it cannot be distinguished anymore. FAD consists of Riboflavin with attached adenosine diphosphate. Hence, it has the same emission signal as Riboflavin. The lower concentration of FAD-molecules compared to Riboflavin lead to poor discrimination of the two analytes.

The limitations of the Pyridoxine detection result from low absorption yields at 280 nm. In addition, the emission signal is partly superimposed by the intense BSA peak. Furthermore, the fluorescence emission of pyridoxine is reabsorbed by riboflavin leading to a further intensity decrease.

In direct comparison, the BioView® measurements resulted in similar RMSEE and RMSEcv values although one additional component was required for the BioView® to reach similar performance (Table 3).

The tests proved the detectability of several in cell cultures relevant fluorophore even in lowest concentrations. The performance was then put to the test in cell cultivations.

3.2 | Cultivations

For further evaluation, the sensor system was set up with a bioreactor, and spectral data was collected every ten minutes during three analogously run CHO-cultivations (K1-K3). This data was then used to build a BEM (Table 4). During these runs, for the first 140 h, the TCC increased to a concentration of up to 32 × 10^6 cells/mL. This occurs in a similar pattern in all three cultivations. During that period, the viability stayed over 90%. Viability starts to decrease after approximately 136 h, until it drops below 60%. At this point the cultivation was stopped. Trajectories of glucose, glutamine and glutamate were also alike during all three cultures. The pattern of the lactate concentration is equal, while the maximal concentration during run K3 only reaches approximately 2.8 g/L, while it goes up to 4.1 g/L in K1 and K2 (Supporting Information Figure 1).

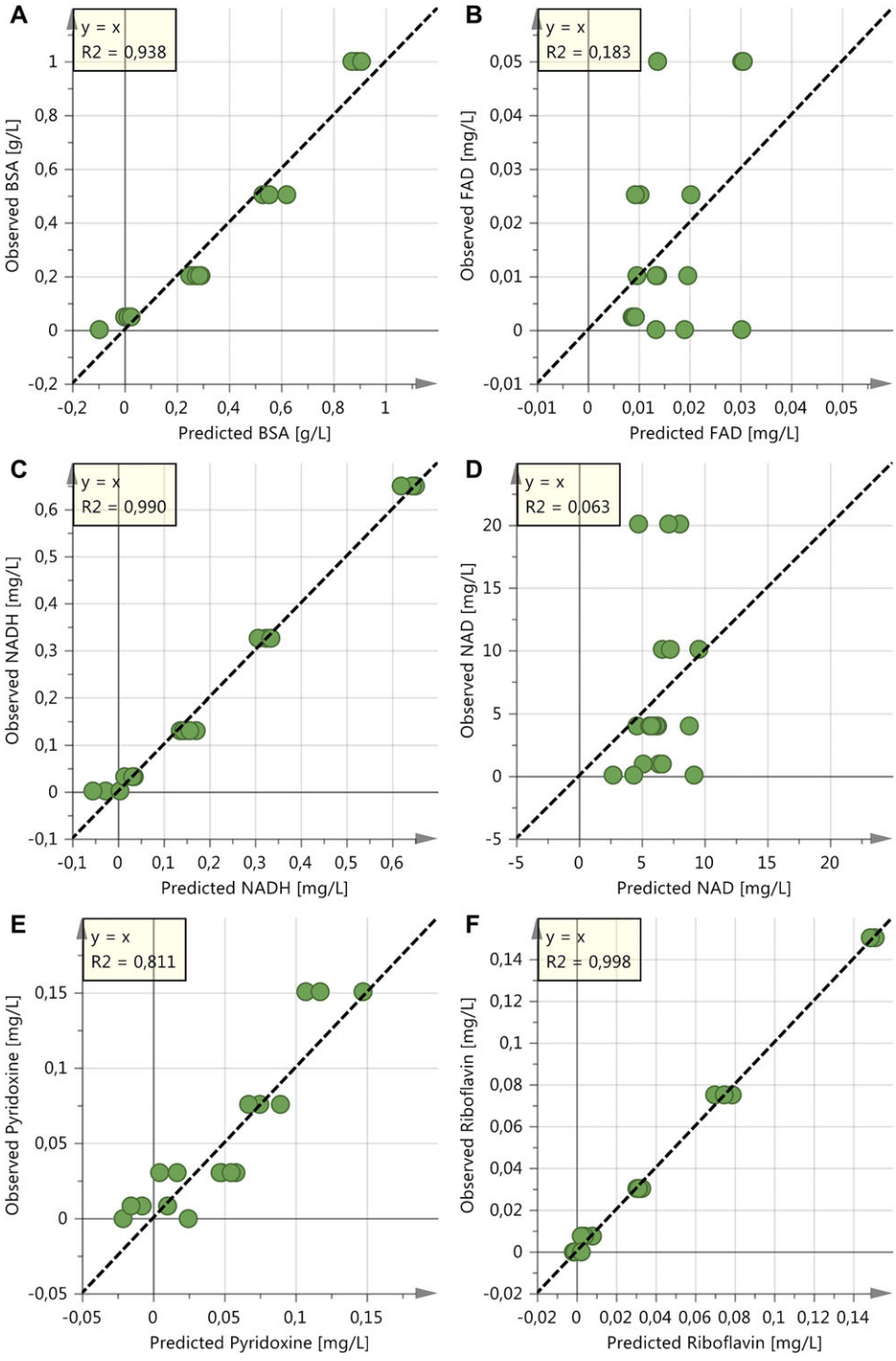

FIGURE 3 Observed versus. predicted plots of each analyte tested in the DoE-Study: (A) BSA, (B) FAD, (C) NADH, (D) NAD, (E) Pyridoxine, (F) Riboflavin

After a first look at the collected raw spectra over time, a distinct pattern that remained similar in each fed batch, was visible. Overall, seven peaks accounted for five different analytes - tyrosine, tryptophan, NADH, pyridoxine and (ribo-) flavins (Figure 4). The two amino acids tyrosine's and tryptophan's fluorescence signal first decreased until the timepoint (~110 h) at which a shift from nutrient to metabolite consumption and decrease in the growth rate occurs (Figure 4), Supporting Information Figure 1. Later the signal increases again. This first decrease is most likely due to utilization of the amino acids by the growing cells for protein production. The lack of nutrients causes decreasing growth rates and thus an accumulation of tyrosine. In addition to the metabolic conversion of phenylalanine to tyrosine, both

TABLE 3 DoE results for each analyte compared between new led-based 2df-system and bioView®

Analyte	LED based # Comp.	R^2y	RMSEE	RMEScv	BioView # Comp.	R^2y	RMSEE	RMSEcv
BSA	1 + 0	0,938	0,0876	0,0865	1 + 1	0,945	0,0849	0,0819
FAD	–	–	–	–	–	–	–	–
NADH	1 + 2	0,99	0,0242	0,0266	1 + 3	0,976	0,0393	0,1141
NAD	–	–	–	–	–	–	–	–
Pyridoxine	1 + 2	0,811	0,0245	0,0357	1 + 3	0,998	0,0089	0,0323
Riboflavin	1 + 0	0,998	0,0026	0,0025	1 + 1	0,997	0,0028	0,0031

TABLE 4 Batch-descriptions of cultivations used for bem building and evaluation

Batch ID	VCC_{Start} [10^6/mL]	VCC_{max} [10^6/mL]	Duration [h]	Feed Strategy	Comment
K1	0.47	30.08	223	Every 24h	Model Building
K2	0.56	32.00	189	Every 24h	Model Building
K3	0.46	26.51	209	Every 24h	Model Building
K4	0.29	25.76	192	Every 24h + Automated Glc	Positive Control
K5	–	13.96	311	Every 24h + Automated Glc	Oxygen Limitation / Negative Control

effects lead to the detected increase of the tyrosine band. Tryptophan, on the other hand, cannot be synthesized by the CHO-cells and can only accumulate from the added medium.

The signal of NADH first increases with a progressively steepening course and then decreases again towards the end of the cultivation when the total cell count starts to decrease as well. Without glucose limitation, CHO cells tend to have an overproduction of NADH which in addition to the general cell growth leads to the ever-increasing production of NADH. Also, when there is a metabolic shift from glucose to lactate consumption by the cells, again NADH is produced by the cells [11]. Whenever the cells start to die off, naturally the production and therefore the presence of NADH decreases as well.

The vitamins pyridoxine and riboflavin, on the other hand, generally decrease over time. As those analytes are only used as a substrate by the cells, this decrease can solely be explained by cellular consumption. Short, small increases can be observed whenever feed-medium is added, as these vitamins are components in it.

From these spectra, first a qualitative PCA-model with three PCs that explains 99.3% of the variance was generated. The score plot of PC 2 versus. PC 1 reveals a distinct pattern, which remains consistent in all three fed-batches (Figure 5). The first turning point corresponds to the batch maturity at which the nutrients glucose and glutamine are exhausted (∼110h), and the metabolic shift towards metabolite consumption like lactate and glutamate occurs. The second turning point occurs around the time that lactate is depleted as well and the TCC starts to decrease (∼190 h) (Supporting Information Figure 1). The second turning point therefore corresponds to the time at which cell lysis occurs and intra-cellular components are released into the medium. Upon investigation of the different loading plots of the first two components, it is revealed that PC 1 is mostly derived from the Rayleigh-backscattering, while PC 2 mostly stems from the intrinsic fluorescence of amino acids and vitamins (Figure 5c). Therefore, it can be assumed that the first component mostly relates to cell growth while the second one relates to cellular metabolism. This is in agreement with previous findings in other studies, e.g., Sandor et al. [12].

The trajectories of the OPLS based batch evolution model follow the same pattern in the score plot. Until the first turning point (corresponding to the time of the first metabolic shift) all trajectories run almost on top of each other. Between first and second turning point the trajectories begin to drift apart. The drift increases with start of apoptosis. This effect is likely due to higher variations introduced by the dying cells. Despite the increasing variations the batch control charts still result in a narrow corridor for the three-sigma limits up to the point at which the TCC starts to decrease (Figure 6). This is a result of the three model batches being reasonably similar as well as the high accuracy and reproducibility of the measurement.

For further comparison to the state-of-the-art, the course of the NADH-associated fluorescence-signal of one cultivation (K1) was compared between the new device and a BioView® sensor. Figure 7 displays the NADH emission over the batch maturity for both systems. The new device showed substantially lower noise, and each feed-addition is easily distinguished from the regular pattern. In contrast, the BioView®'s signal showed much higher noise thus hampering feed detection.

3.3 | Model evaluation

The BEM models were challenged with two additional fed-batches (K4 + K5). In cultivation K4, process control was realized by an automated glucose feed from day four onwards,

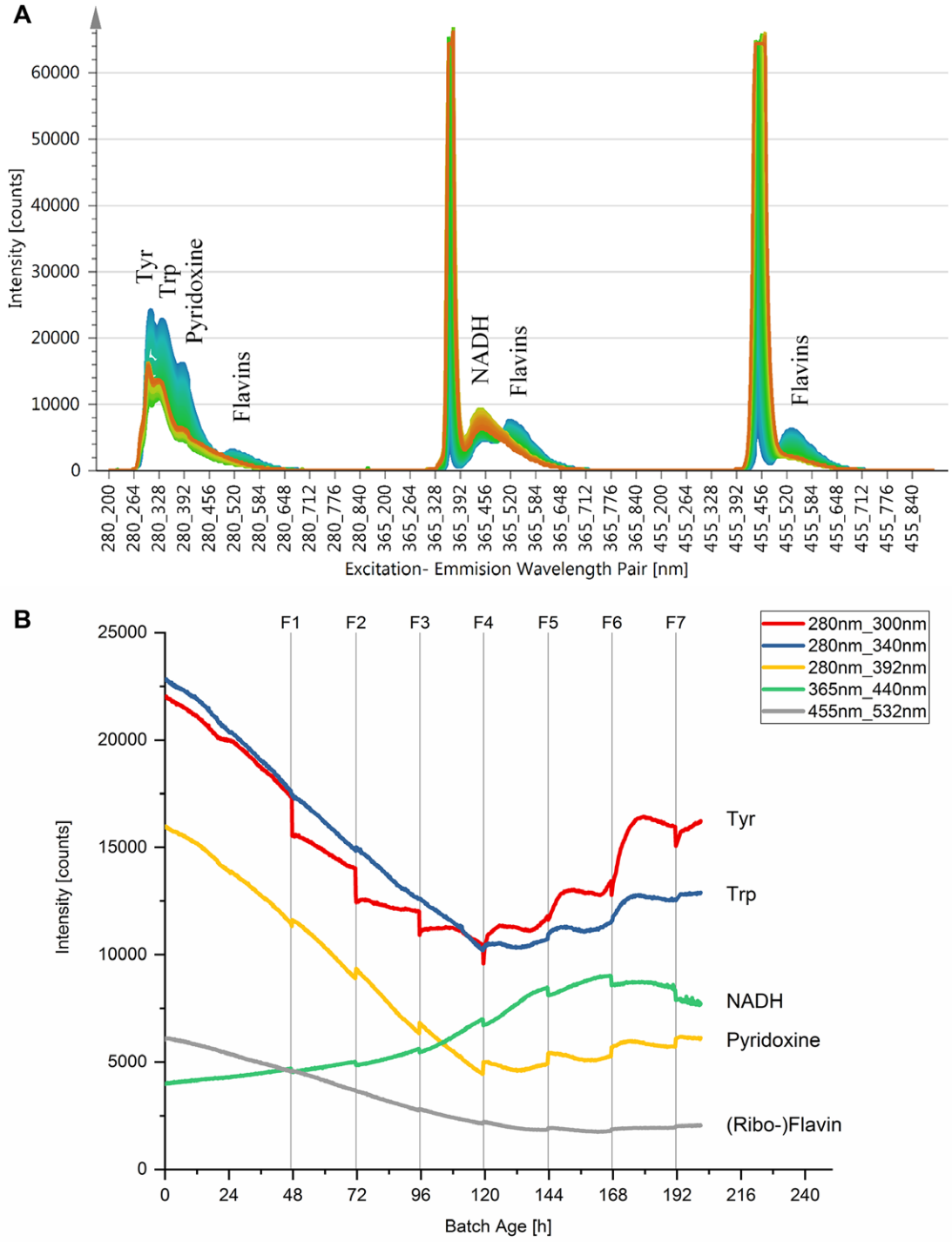

FIGURE 4 (A) Linear fused spectra from cultivation K1, colored according to batch age [h] from Blue (0 h) to Red (250 h); Saturated Raleigh-Wavelengths were excluded for BEM; (B) Time-course of several important excitation-emission wavelength combinations chosen from Figure 4, that can be associated to different Fluorophores; Feeds: F1-F7

in addition to the daily feeds. In the second evaluation culture (K5), the cells were stressed by cutting the airflow for several hours (27–40 h) (Supporting Information Figure 2). It was investigated how fast the sensor detects deviations from regular cultivations (Table 4).

The trajectory of the first control-batch (K4) does not deviate substantially from the "golden"- batch, therefore following the average time-based profile of the previous three cultivations that were used for model-building (Figure 6). This is in good agreement with the qualitative assessment of the batch:

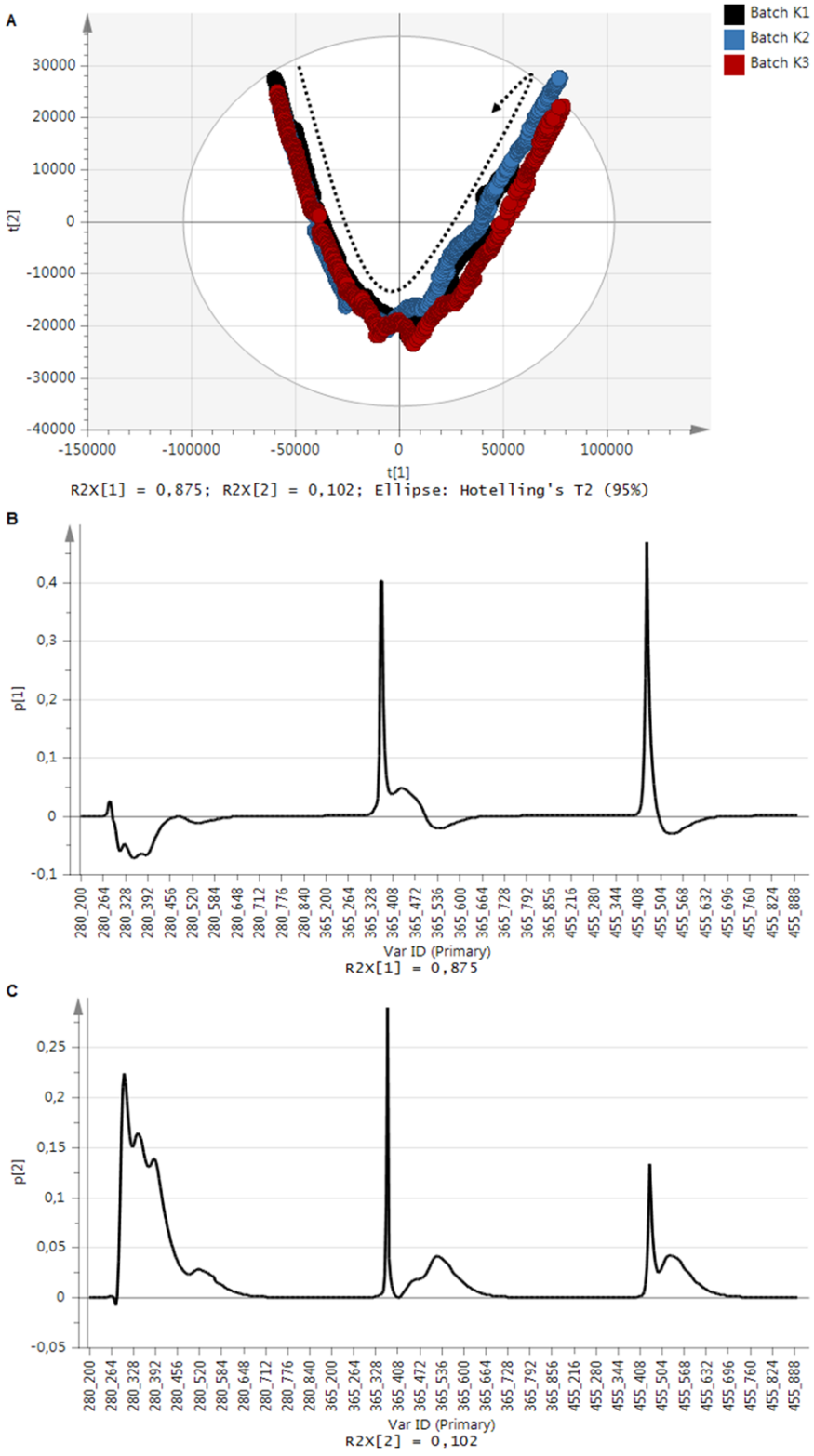

FIGURE 5 (A) Score Plot of PCA-model from cultivations K1-K3 with score t[1] plotted against score t[2]; dotted-arrow indicates course of the batch maturity; (B) loading plot of pc 1 and (C) pc 2 with peaks from the rayleigh-backscattering as well as those stemming from different intrinsic fluorophores

All quality measures were well in between the acceptance criteria, i.e. staying in-between the $\pm 3\sigma$ limits. This is in accordance to the reference analytics that did not detect any significant deviation from the standard batch behavior (Supporting Information Figure 1). In combination with the knowledge gathered previously from investigating the score plot, this can be related to the similar progression of the cell count and a similar point of changing metabolism towards metabolite consumption.

In the second control-batch (K5), the deviation caused by oxygen deprivation is observed. The airflow was cut after around 27 h of cultivation time and recovered approximately

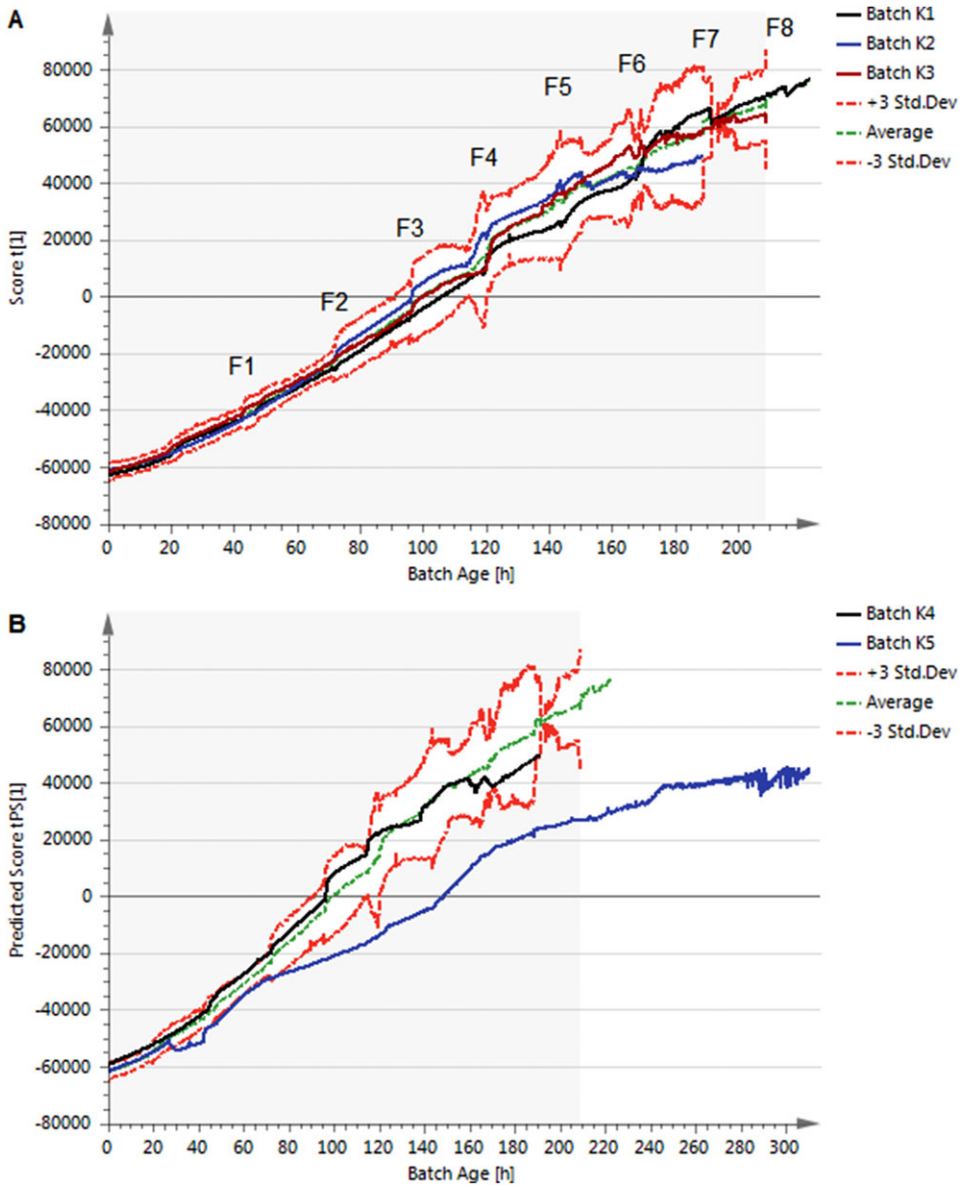

FIGURE 6 (A) Batch Control Chart of Batch Evolution Model made from Cultivations K1-K3 where Principal Component t[1] is plotted against the Batch Age; Dashed green line is the average time-course of the Scores from K1-3; Feeds: F1-8; (B) Prediction Batch Control Chart of K4 and K5 where the Predicted Score tPS[1] is plotted against the Batch Age; Average and ±3 h. Deviation Limits correspond to those from the BEM (Figure 6)

13 h later (Supporting Information Figure 2). The trajectory starts to drift away from the golden batch after approximately half an hour and crosses the -3σ limit after approximately two hours post airflow cut (Figure 6). A comparable offline indicator for the oxidative stress on the cells can be lactate. As no more oxygen is present, only anaerobic glycosylation can occur [13]. This effect can be observed as a sharp increase in lactate concentration in comparison to the regular runs (Supporting Information Figure 1). This deviation in the reference analytics is visible at approximately 35 h batch maturity, and therefore several hours after the fluorescence sensor detected it. The response time of a sensor is a critical factor to enable fast corrective action before critical process deviations occur. In this case, the fluorescence sensor does not just react to the dissolved oxygen outside of the cells, as a pO2-sensor does, but to the stressed state of the cells. In turn, this means the fluorescence sensor can detect cellular changes much faster than any offline readings, hence making it a valuable cell monitoring device.

4 | CONCLUDING REMARKS

This study demonstrated the capabilities of a newly developed 2D-fluorescence system, which aims for the in-line

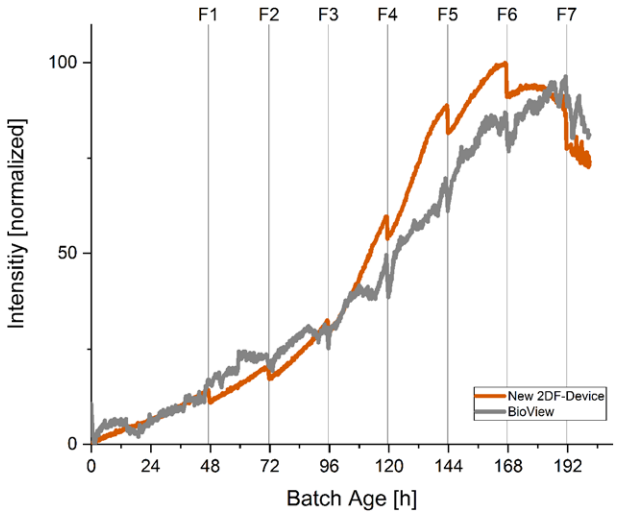

FIGURE 7 Comparison of the NADH-signal courses over time measured with the new 2DF-System brown) and the state-of-the-art BioView® sensor (grey); Feed addition: F1-F7

monitoring of mammalian cell cultures in an industrial production environment.

The combination of high power LEDs with a very sensitive CCD-spectrometer prove to measure in a remarkably reproducible manner. Most intrinsic fluorophores in cell cultivations can be traced with this sensor, which makes it perfect for online monitoring of mammalian cell cultures. The individual probe design and therefore the lack of any filter wheels, multiplexers or other moving parts supports longevity and low-maintenance of the system, thus being suitable for applications industrial environments. Even though the sensor is still in a prototype phase, the modular design and the possibility of custom scripting makes the system highly adaptable to different customer needs. It is also attractive for investigation in other cultivation types, e.g., microbial, where other fluorophores are of interest.

The DoE trials showed that the sensor is suitable for the quantification of several essential fluorophores in process-relevant concentrations. The first inline tests in cell cultivations showed that the system is well able to follow the cells' metabolic and growth state during a batch run. A validation run with oxygen limitation over a period of time proves that the sensor can quickly detect deviations from a regular run. By directly detecting the cell's intracellular distress, and not just outside factors, the sensor is much faster than corresponding offline analytics without taking into account the large time gaps between sampling. Summarizing, the system proved its high suitability for cell culture monitoring. Fast reaction times should further allow for direct process control.

In Part II of this publication, the sensor's capabilities for quantitative prediction of several essential process parameters like viable cell count are investigated to confirm the qualitative findings of this first part. In the future, further tests with a second producing cell line will be conducted to explore if the shown results are transferable and if the target protein concentration can be predicted as well.

ACKNOWLEDGMENTS

This research was supported by the German Federal Ministry of Education and Research (Grant-No. 13N12703). Furthermore, we are thankful for the great support from art photonics (Germany) and J&M Analytik AG (Germany) with the development of the probe and sensor system.

CONFLICT OF INTEREST

The authors have declared no conflict of interest.

ORCID

Alexander Graf https://orcid.org/0000-0002-0401-7470

REFERENCES

1. Classen, J., Aupert, F., Reardon, K. F., Solle, D. et al., Spectroscopic sensors for in-line bioprocess monitoring in research and pharmaceutical industrial application. *Anal. Bioanal. Chem.* 2017, *409*, 651–666.
2. Bakeev, K. A. (Ed.), *Process Analytical Technology: Spectroscopic tools and implementation strategies for the chemical and pharmaceutical industries*, 2nd Ed., John Wiley & Sons, Ltd, Chichester, UK 2010.
3. Faassen, S. M., Hitzmann, B., Fluorescence spectroscopy and chemometric modeling for bioprocess monitoring. *Sensors (Basel, Switzerland)* 2015, *15*, 10271–10291.
4. Zabriskie, D. W., Humphrey, A. E., Estimation of fermentation biomass concentration by measuring culture fluorescence. *Appl. Environ. Microbiol.* 1978, *35*, 337–343.
5. Dickens, J. E., Fluorescent Sensing and Process Analytical Applications, in: Bakeev, K. A. (Ed.), *Process Analytical Technology: Spectroscopic tools and implementation strategies for the chemical and pharmaceutical industries*, 2nd Ed., John Wiley & Sons, Ltd, Chichester, UK 2010, pp. 337–352.
6. Li, B., Shanahan, M., Calvet, A., Leister, K. J. et al., Comprehensive, quantitative bioprocess productivity monitoring using fluorescence EEM spectroscopy and chemometrics. *The Analyst* 2014, *139*, 1661–1671.
7. Hantelmann, K., Kollecker, M., Hüll, D., Hitzmann, B. et al., Two-dimensional fluorescence spectroscopy: A novel approach for controlling fed-batch cultivations. *J. Biotechnol.* 2006, *121*, 410–417.
8. Moe, A. E., Marx, S., Banani, N., Liu, M. et al., Improvements in LED-based fluorescence analysis systems. *Sens. Act. B: Chem.* 2005, *111–112*, 230–241.
9. Marose, S., Lindemann, C., Scheper, T., Two-dimensional fluorescence spectroscopy: A new tool for on-line bioprocess monitoring. *Biotechnol. Prog.* 1998, *14*, 63–74.
10. Siegel, J. M., Montgomery, G. A., Bock, R. M., Ultraviolet absorption spectra of DPN and analogs of DPN. *Archives of Biochem. Biophys.* 1959, *82*, 288–299.

11. Nolan, R. P., Lee, K., Dynamic model of CHO cell metabolism. *Metabol. Eng.* 2011, *13*, 108–124.
12. Sandor, M., Rüdinger, F., Bienert, R., Grimm, C. et al., Comparative study of non-invasive monitoring via infrared spectroscopy for mammalian cell cultivations. *J. Biotechnol.* 2013, *168*, 636–645.
13. Handlogten, M. W., Zhu, M., Ahuja, S., Intracellular response of CHO cells to oxidative stress and its influence on metabolism and antibody production. *Biochem. Eng. J.* 2018, *133*, 12–20.
14. Richards-Kortum, R., Sevick-Muraca, E., Quantitative optical spectroscopy for tissue diagnosis. *Ann. Rev. Phys. Chem.* 1996, *47*, 555–606.
15. Li, J. K., Humphrey, A. E., Use of fluorometry for monitoring and control of a bioreactor. *Biotechnol. Bioeng.* 1991, *37*, 1043–1049.
16. Wolfbeis, O. S., *The fluorescence of organic natural products*, Wiley, New York NY. 1985.
17. Bottiroli, G., Croce, A. C., Locatelli, D., Marchesini, R. et al., Natural fluorescence of normal and neoplastic human colon: A comprehensive "ex vivo" study. *Lasers Surg. Med.* 1995, *16*, 48–60.
18. Fluorophores.org [Internet] [cited 2018 Apr 16]. Available from: http://www.fluorophores.tugraz.at/.
19. Li, Y., Silva, P. G., de, Xi, L., van Winkle, A. et al., Separation of flavins and nicotinamide cofactors in Chinese hamster ovary cells by capillary electrophoresis. *Biomed. Chrom.: BMC* 2008, *22*, 1374–1384.
20. Huhner, J., Ingles-Prieto, A., Neususs, C., Lammerhofer, M. et al., Quantification of riboflavin, flavin mononucleotide, and flavin adenine dinucleotide in mammalian model cells by CE with LED-induced fluorescence detection. *Electrophoresis* 2015, *36*, 518–525.
21. Ghorbaniaghdam, A., Henry, O., Jolicoeur, M., A kinetic-metabolic model based on cell energetic state: Study of CHO cell behavior under Na-butyrate stimulation. *Bioprocess and Biosystems Eng.* 2013, *36*, 469–487.

SUPPORTING INFORMATION

Additional supporting information may be found online in the Supporting Information section at the end of the article.

How to cite this article: Graf A, Claßen J, Solle D, Hitzmann B, Rebner K, Hoehse M. A novel LED-based 2D-fluorescence spectroscopy system for in-line monitoring of Chinese hamster ovary cell cultivations – Part I. *Eng Life Sci* 2019;19:352–362. https://doi.org/10.1002/elsc.201800149